

Design and Demonstration of the “Flow-Cell” Integrated-Flow, Active-Cooling Substrate for High-Average-Power Substrates

E. P. Power, S. Bucht, K. R. P. Kafka, J. Bromage, and J. D. Zuegel

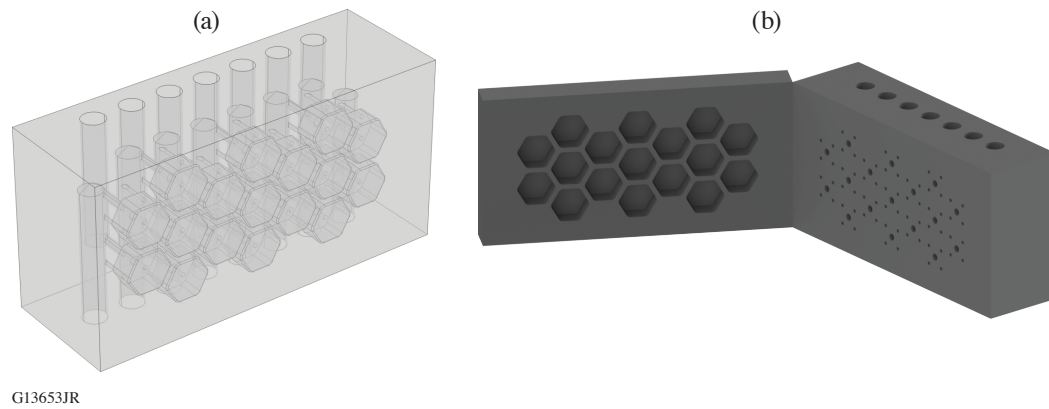
Laboratory for Laser Energetics, University of Rochester

We designed, fabricated, and tested a prototype flow-cell integrated-cooling substrate built using cordierite ceramic and demonstrated average power handling up to 3.88-W/cm^2 absorbed power density with 54-nm peak-to-valley deformation in a sub-aperture test.^{1,2} Mechanical stabilization was observed to occur on a time scale <30 s. Model predictions indicate a full-aperture performance limit of 2.6-W/cm^2 absorbed power density with $<\lambda/10$ deformation and <90 -s stabilization time, equivalent to 100-mJ/cm^2 fluence per pulse with a 1-kHz repetition rate on an optic with 2.6% absorption. Chirped-pulse–amplification lasers commonly use gold-coated compressor gratings operating with beam-normal fluences of $\sim 100\text{ mJ/cm}^2$ to stay below the short-pulse damage-fluence limit. Existing multiterawatt and petawatt femtosecond lasers operate at relatively low repetition rate (Hz and slower); thermal effects are not experienced by gratings located in vacuum chambers at these low-average powers. Thermal expansion of gratings under high-average-power conditions will cause wavefront deformation (focusing errors) and modify the frequency-dependent path lengths through the system (compression errors), leading to unacceptable spatial and temporal degradation of the focused laser spot and compressed pulse, respectively. Joule-class lasers operating at kilowatt average powers would require large beam sizes ($\sim 300\text{ cm}^2$ or $\sim 20\text{ cm}$ diam) with current gratings given their $\sim 10\text{-W/cm}^2$ average power ($\sim 10\text{ mJ/cm}^2$ at 1 kHz) handling capacity. Simulations show that new gratings fabricated on thermally stable and actively cooled substrates can reduce pulse width, improve temporal contrast, and decrease focal-spot degradation,³ but significantly better thermal management of diffraction gratings is needed for future high-average-power lasers for accelerator and beam-combining applications.

The flow-cell integrated active-cooling design is built around a hexagonal unit cell. The close-packed structure of cells is similar to lightweighted optics for aerospace applications, the primary differences being a closed back and integrated fluid input/output channels. The final prototype design uses a hexagon inscribed in a 13-mm diameter with 8-mm pocket depth and cell-to-cell wall thickness of 2 mm. Exterior dimensions for the prototype are $130.18 \times 63.5 \times 47.29\text{ mm}^3$, with a defined clear aperture of $101.6 \times 50.8\text{ mm}^2$ centered on the front surface. The front boundary of each cell is located 5 mm behind the optical surface. Figure 1 shows the interior structure of the fabricated prototype.

COMSOL modeling was performed using unidirectional coupling between pressure in the fluid domain and deformation in the solid domain. That is, it was assumed that the small nanometer-scale motion of the fluid–solid boundaries would not impact fluid flow, which is defined by millimeter-scale geometric features. Therefore, as discussed in more detail in Ref. 1, steady-state isothermal turbulent flow was computed once, and the resulting fluid velocities and pressures were used as static input to the follow-up thermomechanical computation. The predicted temperature rise of $<1^\circ\text{C}$ in the fluid is assumed insufficient to require a fully coupled model including non-isothermal flow. Input and output coolant baths were computed only in the fluid domain; we are uninterested in the response of the steel plenum pieces fabricated as dual-purpose optic mount/fluid baths.

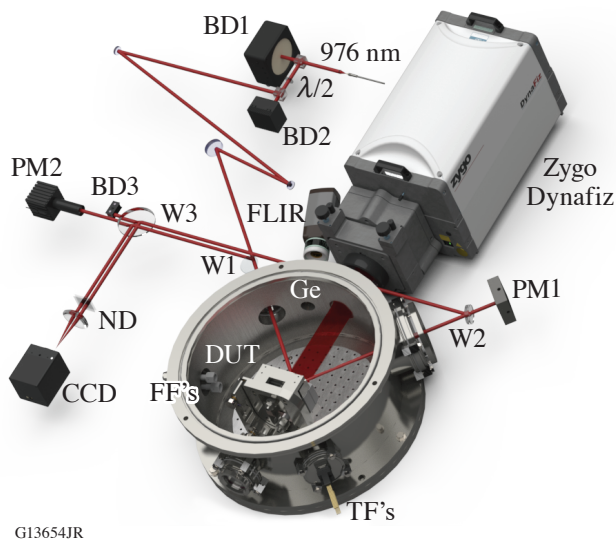
Figure 2 shows the heater beam delivery and metrology for testing thermally loaded samples. The device under test was held under vacuum in a custom-built cylindrical vacuum chamber. The heater beam entrance and exit ports were arranged 90° apart, allowing 45° incidence on the test optic. The heater source available in our setup was a 976-nm cw source with a maximum on-target power of $\sim 100\text{ W}$. A commercial Fizeau interferometer (Zygo Dynafiz) was used at normal incidence using a 632.8-nm



G13653JR

Figure 1

(a) Transparent rendering of the prototype optic used in modeling. The optical surface is toward the front, fluid input is through the top columns, and coolant drainage is through the bottom (obscured). (b) Opaque rendering of the prototype optic cut open at the back plane of the flow cells to aid visualizing input and output channels for individual unit cells.



G13654JR

Figure 2

Thermal loading test stand layout using the 976-nm heater source. BD1: water-cooled beam dump; BD2, BD3: air-cooled beam dumps; W1, W2, W3: uncoated wedges; PM1: water-cooled thermopile; PM2: air-cooled Si diode + integrating sphere; FF: fluid feedthrough; TF: thermocouple feedthrough; ND: neutral-density filter; CCD: charge-coupled device; DUT: device under test. A Ge window for the FLIR thermal imaging camera is shown; all other windows are V-coated for the appropriate wavelength (976-nm heater or 632.8-nm Fizeau).

stabilized HeNe laser. A small Ge window placed near the interferometer window allows a thermal imaging camera (FLIR) to view the heated area. Eight type-K thermocouple feedthroughs allowed for spot measurement of temperature in a variety of locations on the sample, mount, or chamber. Two fluid feedthroughs allowed coolant flow for in vacuum liquid-cooled components.

Cordierite ceramic was selected as the material for the flow-cell prototype due to its superior thermomechanical properties: 4.0 W/m-K thermal conductivity and $<0.02 \times 10^{-6} \text{ K}^{-1}$ thermal expansion coefficient. Steady-state and time-dependent testing of a flow-cell prototype was performed using 97.1 W of optical power, corresponding to 3.88 W/cm^2 absorbed power density. The incidence angle in the COMSOL model was set to 45° to match laboratory conditions. Unfortunately, the 976-nm laser source does not have additional power available; therefore, the beam size could not be increased to cover a larger portion of the clear aperture. Results measured when heating the flow-cell with 3.88 W/cm^2 absorbed power density are shown in Figs. 3(a) and 3(c), with COMSOL model results in Fig. 3(b). Agreement between the modeled and measured steady-state response in Figs. 3(b) and 3(c) is excellent, differing by 0.2 nm peak-to-valley (p-v). Also in excellent agreement is the time-dependent response in Fig. 3(a); stabilization dynamics measured in the laboratory are well matched by model predictions, and the observed mechanical stabilization time is $<30 \text{ s}$ to reach $>99\%$ of the steady-state deformation.

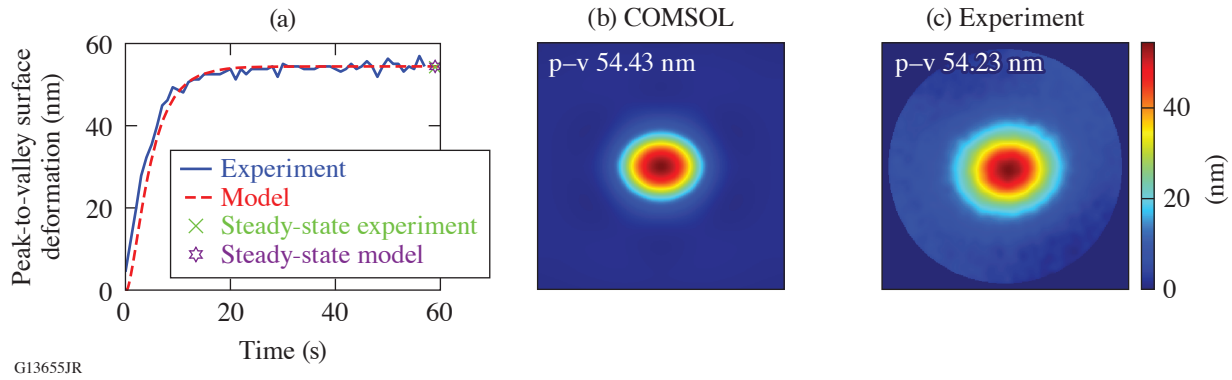


Figure 3

(a) Stabilization dynamics of the flow-cell prototype as indicated by the measured p–v surface deformation (blue curve): the sample was heated with a 1.3-cm-diam beam with absorbed power density of 3.88 W/cm^2 . Surface maps were acquired in fast Fizeau mode at 1 Hz; $t = 0$ marks the initiation of the heater beam. Model results for the same conditions (red curve) are an excellent match; the dynamics and stabilization time scales are well reproduced. Mechanical stabilization was observed to occur in $<30 \text{ s}$. (b) COMSOL steady-state model prediction for surface deformation, and (c) measured surface deformation after 5 min of continuous heating.

We used the same COMSOL model that successfully predicted sub-aperture behavior to predict full-aperture performance. The only model parameters changed were beam diameter (increased to 5 cm) and optical power (increased to 1 kW). The resulting absorbed power density was 2.6 W/cm^2 , slightly above our 2.5-W/cm^2 design target. Figure 4 shows the results from this modeling effort: (a) shows that the thermal profile is qualitatively similar to the sub-aperture case we tested in the laboratory, with peak temperature on the surface slightly lower in this scenario due to the lower absorbed power density, and (b) shows the surface deformation dynamics: surface deformation reaches $>99\%$ of the steady-state value in $<90 \text{ s}$. The steady-state model predicts 80-nm deformation for 2.6-W/cm^2 absorbed power density, meeting the $\lambda/10$ limit at 800 nm.

We simulated the dynamic response of a passively cooled cordierite brick with identical outer dimensions and beam geometry as the flow-cell prototype and found an upper limit of $\sim 0.1 \text{ W/cm}^2$ absorbed power density to maintain p–v deformation $< \lambda/10$. As expected, stabilization was orders of magnitude slower, reaching the $>99\%$ threshold for p–v deformation required 4.75 h, as shown in the inset of Fig. 4(b).

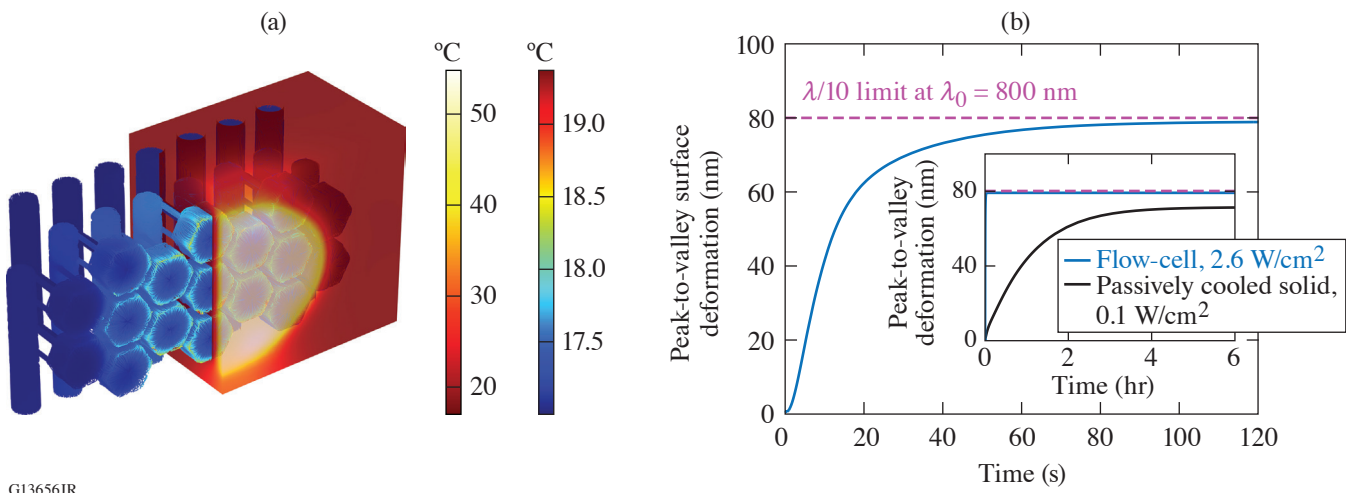


Figure 4

COMSOL results for the flow-cell prototype heated with a 5-cm-diam beam. (a) Temperature profile using 2.6-W/cm^2 absorbed power density; the solid domain is semi-transparent. (b) Predicted heating dynamics: the mechanical stabilization time was $<90 \text{ s}$. Inset: dynamic response of a passively cooled cordierite brick heated with 0.1 W/cm^2 .

In separate testing, Plymouth Grating Labs fabricated four Au-coated gratings on cordierite coupons, as well as two reference gratings on fused silica. Diffraction efficiency and laser-damage–threshold measurements for test gratings fabricated on cordierite coupons reveal no red flags, with average efficiencies of 88.4%, 89.9%, 91.5%, and 91.7%; all measurements were made at 799 nm. Despite higher-amplitude content in polished cordierite 1-D power spectral densities, diffraction efficiency measurements of the best two gratings on cordierite are within 1% of witness gratings on glass, and 50-on-1 laser-damage threshold is identical at 250 mJ/cm² for both glass and cordierite gratings.

This material is based upon work supported by the Department of Energy Office of Science under Award Number DE-SC0019496, the University of Rochester, and the New York State Energy Research and Development Authority.

1. E. P. Power *et al.*, Opt. Express **30**, 42,525 (2022).
2. E. P. Power *et al.*, “Demonstration of the “Flow-Cell” Integrated-Flow Active Cooling Substrate for High-Average-Power,” submitted to Optics Letters.
3. D. A. Alessi *et al.*, Opt. Express **24**, 30,015 (2016).